A database of validation cases for tsunami numerical modelling

Damien Violeau, Riadh Ata, Michel Benoit, Antoine Joly, Stéphane Abadie, Lucie Clous, Manuel Martin Medina, Denis Morichon, Jérémie Chicheportiche, Marine Le Gal, et al.

A database of validation cases for tsunami numerical modelling

D. Violeau, R. Ata, M. Benoit[(1)], A. Joly
EDF and Saint-Venant Hydraulics Laboratory, Chatou, France
[(1)]Now at IRPHE and Ecole Centrale Marseille, Marseille, France

S. Abadie, L. Clous, M. Martin Medina, D. Morichon
Université de Pau et des Pays de l'Adour, Anglet, France

J. Chicheportiche, M. Le Gal
Ecole des Ponts ParisTech, Marne-la-Vallée, France

A. Gailler, H. Hébert, D. Imbert
CEA, DIF, DAM, Arpajon, France

M. Kazolea, M. Ricchiuto
Team CARDAMOM, Inria Bordeaux sud-Ouest, Bordeaux, France

S. Le Roy, R. Pedreros, M. Rousseau
BRGM, Orléans, France

K. Pons, R. Marcer, C. Journeau
Principia, La Ciotat, France

R. Silva Jacinto
Ifremer, Géosciences Marines, Centre de Brest, France

ABSTRACT: This work has been performed by a French national consortium within the framework of the national project Tandem, with aim to improve knowledge about tsunami risk on the French coasts. Work-package #1 of this project was the opportunity to build a database of benchmark cases to assess the capabilities of 18 codes, solving various set of equations with different numerical methods. 14 test cases were defined from the existing literature with validation data from reference simulations, theoretical solutions or lab experiments. They cover the main stages of tsunami life: 1) generation, 2) propagation, 3) run-up and submersion, and 4) impact. For each case several of the numerical codes were compared in order to identify the forces and weaknesses of the models, to quantify the errors that these models may induce, to compare the various modelling methods, and to provide users with recommendations for practical studies. In this paper, 3 representative cases are selected and presented with an analysis of the results.

1 INTRODUCTION

This work has been performed by a French national consortium within the framework of the national project Tandem (2014-2017), with aim to improve knowledge about tsunami risk on the French coasts. The first of the four work-packages of the Tandem project (WP1 – Qualification and validation of numerical codes) was the opportunity to build a database of benchmark cases to assess the capabilities of various (industrial or academic) numerical codes.

18 codes were used, solving various set of equations with different numerical methods. 14 test cases were defined from the existing literature with validation data from reference simulations, theoretical solutions or lab experiments. They cover the main stages of tsunami life: 1) generation (from seism or landslide), 2) propagation, 3) run-up and submersion, and 4) impact. For each case several of the numerical codes were compared in order to identify the forces and weaknesses of the models, to quantify the errors that these models may induce, to compare the various modelling methods, and to provide users with recommendations for practical studies. Here, 3 representative cases are selected and detailed with an analysis of the results:

- Case GG07: "Russel's wave generator",
- Case P02: "Solitary wave reflecting on a 2D vertical reef",
- Case RS04: "Seaside experiment: impact on a urban area".

These cases have been chosen as being representative of the main phases of tsunami life, while being simulated by a significant number of codes from the project's list. The participants to Tandems's WP1 are the French institutes listed below:

- CEA (Commissariat à l'Energie Atomique), public research institute, Project coordinator,
- EDF (Electricité de France), private company, WP1 coordinator,

– UPPA (Université de Pau et des Pays de l'Adour), academic institution,
– ENPC (Ecole des Ponts ParisTech), academic institution,
– Inria, public research institute,
– BRGM (Bureau de Recherches Géologiques et Minières), public research institute,
– Principia (French), private engineering company,
– Ifremer (Institut Français pour la Recherche et l'Exploitation de la Mer), public research institute.

It is noted that on the P02 test selected here the waves are propagated on rather short distances; cases with long distance propagation of solitary-type waves or initial disturbances are also included in the test bed.

2 RUSSEL'S WAVE GENERATOR

2.1 *Case description*

This case is the generation of a solitary wave induced by the vertical fall of a rectangular rigid body and its interaction with the underlying water body. It is based on the experiment published in Monaghan and Kos (1999). This benchmark allows checking the accuracy of a model in a case of strong interactions of a rigid body with free surface. It involves interface reconnections and vortices generation and thus requires the use of models able to deal with these kind of phenomena. In terms of engineering relevance, this case is close to the physics involved in massive cliffs or ice bodies fall into water.

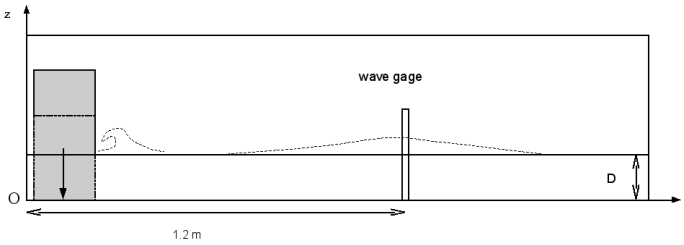

Figure 1. Russel's wave generator: sketch of the experimental apparatus.

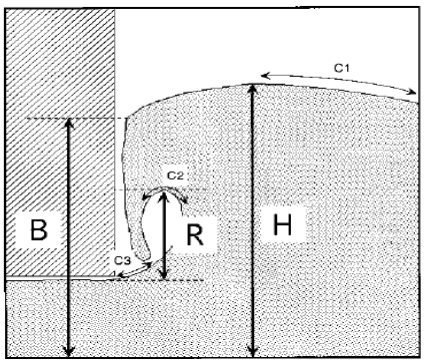

Figure 2. Russel's wave generator: definitions of *B* and *H* (picture from Monaghan and Kos, 1999).

Fig. 1 represents a sketch of the experiment performed by Monaghan and Kos (1999). The experiment was carried out in a 9m long 2D flume, with water depth *D*. A 38.2kg rectangular block (0.4m tall, 0.3m long and 0.39m wide) is placed just above still water level at initial time, and then released. Experiments were repeated for *D* = 0.288m, 0.210m, and 0.116m; in each case, the block vertical position and free surface elevation were measured as a function of time at a wave gage located 1.2m from the leftward extremity of the flume. Values of *H* and *B* (Fig. 2) were also estimated from video measurements.

To closely reproduce these experiments, in which the block was forced to have a vertical motion, horizontal block velocities must be set to zero in the model. The block has also to be slightly shifted rightward (by 20mm) as in the experimental set-up, and initially positioned 5mm below the free surface.

2.2 *Benchmarking results*

Three Navier-Stokes models are tested here:
– the code THETIS (developed by laboratoire Trèfle, Bordeaux), based on Finite Volume (FV) with the Volume Of Fluid (VOF) technique for free surface tracking,
– the code EOLE, developed by Pincipia, based on FV and VOF as well,
– the code Sphynx, developed by EDF with help from ENPC, based on the Smoothed Particle Hydrodynamics (SPH) method.

To solve the fluid solid interaction, EOLE and Sphynx calculate the resulting pressure force and deduce the motion from Newton's law, while THETIS uses a penalization of viscosity to model the interaction at once.

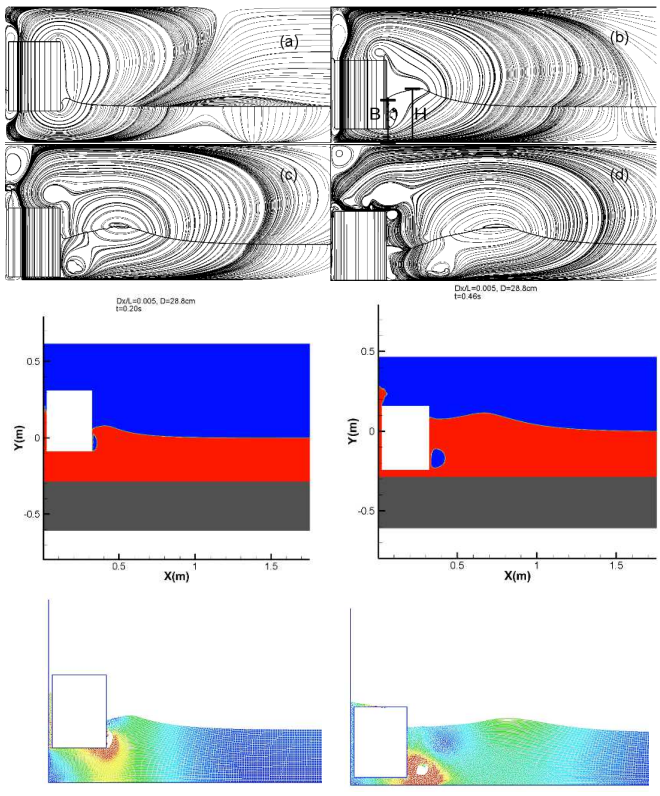

Figure 3. Russel's wave generator: snapshots of simulations with THETIS, EOLE and Sphynx (from top to bottom).

The following discretizations were used in these simulations (L = length of the rigid body):

- THETIS_1: $\delta x/L = 0.02$,
- THETIS_2: $\delta x/L = 0.01$,
- THETIS_3: $\delta x/L = 0.005$,
- EOLE_1: $\delta x/L = 0.01$,
- EOLE_2: $\delta x/L = 0.005$,
- Sphynx: $\delta x/L = 0.016$,

where δx is the mesh (FV) or particle (SPH) size.

Fig. 3 presents snapshots of simulations carried out with the different models. The key point is the accuracy with which the solid motion is simulated. Fig. 4 presents a comparison of the models on this aspect (the curve is to be read from right to left with increasing time). Both VOF models give satisfactory results while the SPH model slightly underestimates velocity at the end of the motion.

Table 1 summarizes the wave height simulated by the models a few solid lengths away from the source position, with various initial water depths. Relative errors are also presented. Experimental values are given with a relatively coarse resolution of 0.01m which prevent from an accurate estimation of the numerical error. Model errors obtained with comparable mesh resolution are presented in bold in the table. The numerical estimations generally show a very good accuracy (within the experimental error bar) except for one simulation per model.

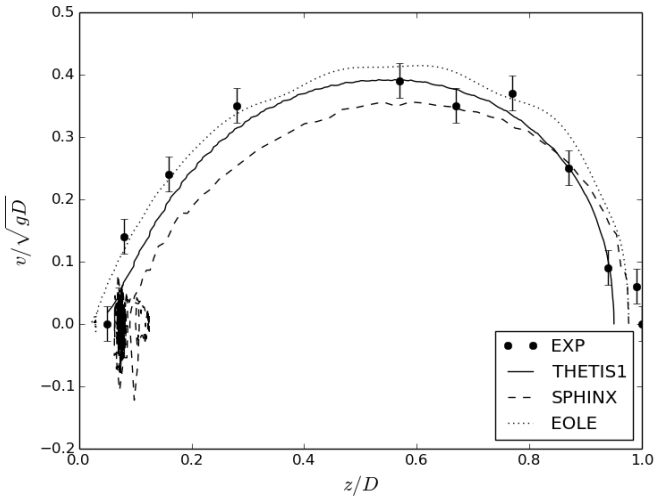

Figure 4. Russel's wave generator: solid velocity versus solid vertical position. Initial water depth = 0.21m. Symbols: experiments from Monaghan and Kos (1999); lines: simulations.

Table 2 presents a comparison of the models estimation of free surface shape close to the solid motion for an initial depth of 0.210m. This table has of course less importance than the preceding one in terms of applications. Here again the results obtained by the models are satisfactory with almost all the predictions within the experimental resolution.

We conclude that the Navier-Stokes models considered in this project are all able to model with a good accuracy the waves generated by a rigid body vertically falling into water taking into account the fluid/solid interaction. It is likely that the conclusion would be the same or not too different for a body entering water with an angle.

Table 1. Russel's wave generator: wave height (m) calculated versus measured at x = 1.2m from the left end of the channel for various water depths.

	D (m)		
	0.116	**0.210**	**0.288**
Experiment	0.109	0.092	0.093
THETIS_1		0.0966	
Error (%)		5	
THETIS_2	0.0967	0.1092	0.1024
Error (%)	**11**	**19**	**10**
THETIS_3		0.100	
Error (%)		10	
EOLE_1	0.085	0.094	0.098
Error (%)	**22**	**2**	**5**
EOLE_2	0.093	0.094	0.101
Error (%)	15	2	9
Sphynx	0.094	0.092	0.092
Error (%)	**14**	**0**	**1**

Table 2. Values of H and B for an initial depth of 0.210m (see Fig. 2).

	H (m)	B (m)
Experiment	0.333 ± 0.01	0.303 ± 0.02
THETIS_1	0.295	0.264
Error (%)	11	13
THETIS_2	0.294	0.270
Error (%)	**12**	**11**
EOLE_1	0.317	0.291
Error (%)	**5**	**4**
EOLE_2	0.317	0.296
Error (%)	5	2
Sphynx	0.295	0.280
Error (%)	**11**	**8**

3 SOLITARY WAVE REFLECTING ON A 2D VERTICAL REEF

3.1 *Case description*

This benchmark aims at reproducing a set of experiments carried out at the O.H. Hinsdale Wave Research Laboratory, Oregon State University (OSU, see Roeber, 2010 and Roeber and Chung, 2012). These experiments involve the propagation, run-up, overtopping and reflection of high amplitude solitary waves on two-dimensional reefs. Their purpose is on one hand to investigate processes related to breaking, bore formation, dispersion, and passage from sub- to super-critical flows, while providing, on the other hand, data for the validation of near-shore wave models in fringing reef.

The geometry of the test considered here is shown on Fig. 5. The length of the basin is of 104m, however the computational domain is delimited by a reflecting wall placed at x = 83.7m. The reef starts at x = 25.9m with a nominal slope of 1/12. The actual slope is such that the height of 2.36 m is reached after 28.25 m. At this station a 0.2m height crest is

mounted. The offshore slope of the crest is the same of the reef, and the length of its plateau is of 1.25m. The on-shore side has a slope of 1/15 giving a nominal length for the crest basis of 6.65 m (using the actual offshore slope, a crest basis of 6.64407 m is obtained). For the computations, the use of the nominal slope values is prescribed. This gives an offshore length of the crest slope (starting at 28.25m) of 2.4m.

The initial depth at still water is taken to be h_0 = 2.5m, giving a partially submerged crest, and a depth behind it (on-shore side) of 0.14m. The initial solution consists of a solitary wave of amplitude A = 0.75m, giving a nonlinearity ratio of A/h_0 = 0.3. To simplify the boundary conditions, the solitary is placed initially at x = 17.6m which is in reality where the experimental data places the peak at dimensionless time $t\sqrt{(g/h_0)}$ = 47.11. This shift will have to be applied consistently when comparing with experiments. Reflective walls are specified at both ends of the computational domain: x = 0 m and x = 83.7 m.

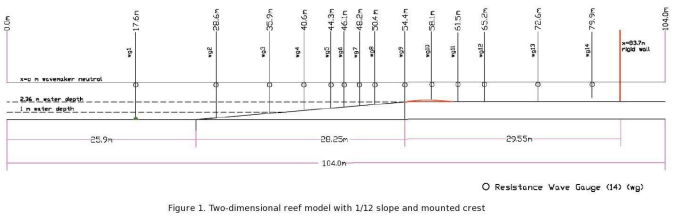

Figure 5. Solitary wave reflecting on a 2D vertical reef: case geometry.

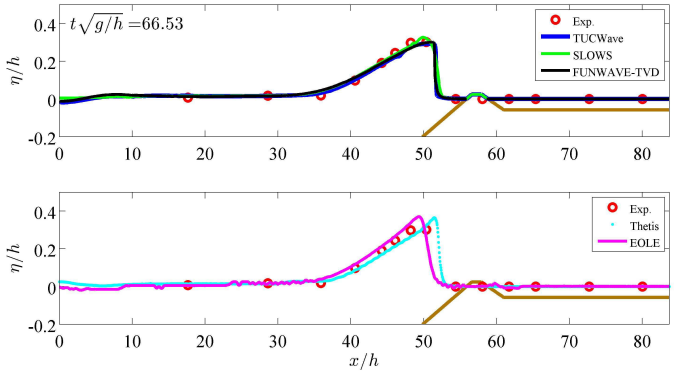

Figure 6a. Solitary wave reflecting on a 2D vertical reef: free surface distribution at non-dimensional time = 66.53. Top: Boussinesq-type models; bottom: Navier-Stokes codes.

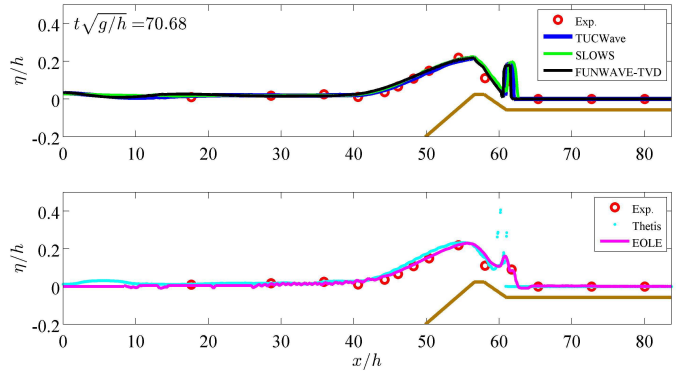

Figure 6b. Continuation of Fig. 6a, non-dimensional time = 70.68.

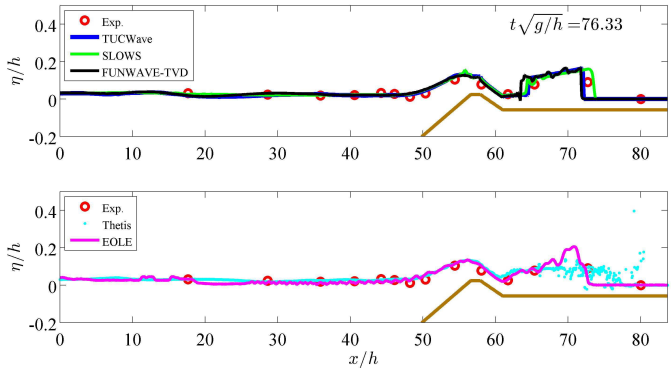

Figure 6c. Continuation of Fig. 6b, non-dimensional time = 76.33.

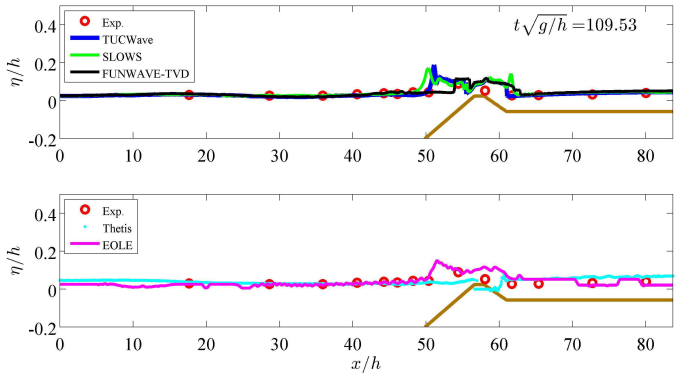

Figure 6d. Continuation of Fig. 6c, non-dimensional time = 109.53.

The prescribed value of the mesh size is 0.05m. A Courant number of 0.4 is imposed. For the friction model, a Manning coefficient of 0.014 $m^{-1/3}$.s is chosen.

3.2 *Benchmarking results*

For this test numerical results are available from the following models:

- THETIS (see Section 2.2),
- EOLE (see Section 2.2),
- TUCWave (Kazolea *et al.*, 2012), developed by Inria and Technical University of Crete, solving hybrid Boussinesq/ Non-Linear Shallow Water Equations (NLSWE) with FV,
- SLOWS (Ricchiuto & Filippini, 2014), developed by Inria, solving hybrid fully nonlinear Green-Naghdi/ NLSWE with a stabilized Finite Elements (FE) approach,
- FUNWAVE-TVD (Shi *et al.*, 2012), developed by Delaware University and Rhode Island University (US), solving hybrid fully nonlinear Boussinesq/NLSWE with structured meshes.

Figs. 6a to 6d compare the measured and computed wave profiles for all numerical models as the numerical solitary wave propagates. Until the dimensional time t^* = 54.91, the initially symmetric solitary wave propagates onshore, shoals across the toe of the slope at x = 25.9 m, due to the inclined bathymetry, and begins to skew to the front. As a result of shoaling the wave breaks around t^* = 59.3 forming a plunging breaker. We can see that the numerical re-

sults of all models are different during the breaking process. TUCWave, SLOWS, and FUNWAVE mimic the breaker as a collapsing bore that slightly underestimates the wave height but conserves the total mass. EOLE and THETIS overestimate the wave height, with a delay in the overall process observed with THETIS (though we do not know the behavior of the free surface between two measurement data points).

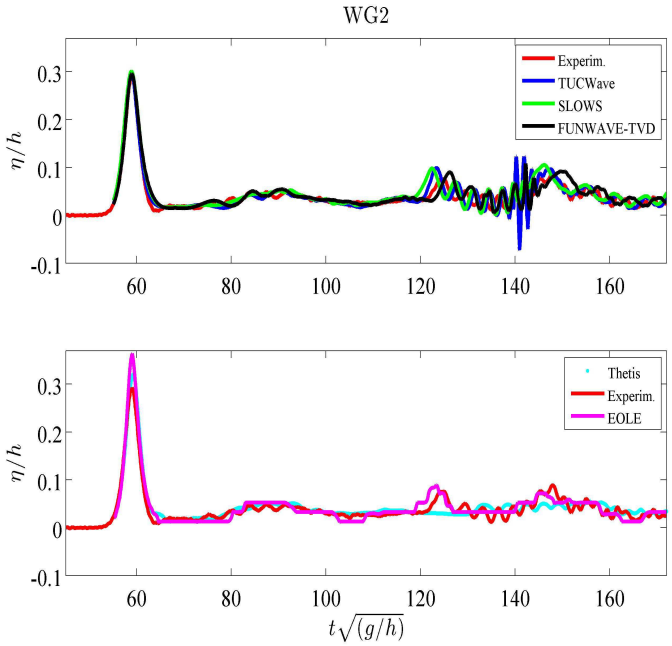

Figure 7a. Solitary wave reflecting on a 2D vertical reef: time series of the normalized free surface at wave gauge (WG) 2. Top: Boussinesq-type models; bottom: Navier-Stokes codes.

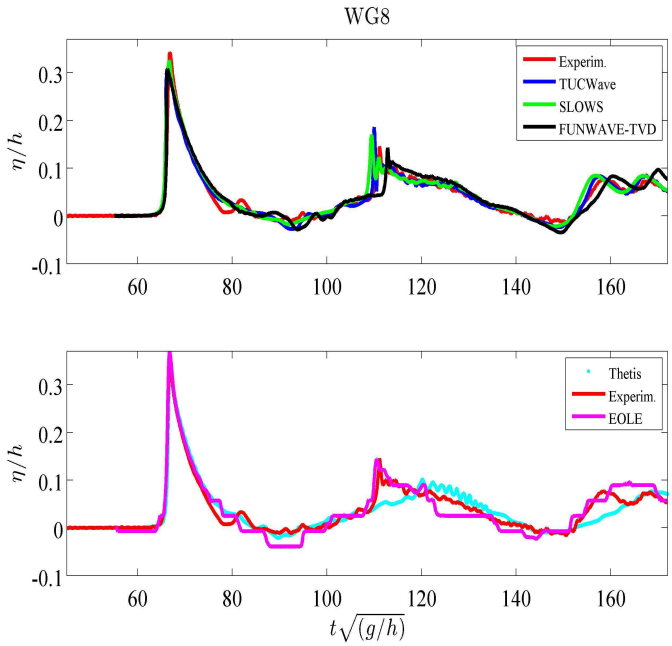

Figure 7b. Continuation of Fig. 7a, WG 8.

The broken wave propagates on the back slope of the reef generating a super-critical flow moving into the stagnant region on the flat reef. While the bore propagates downstream a hydraulic jump develops at the back of the reef. The Boussinesq codes seem to capture this process in a stable manner. After the overtopping of the reef by the reflected bore, we can see the formation of an undular structure, whose inceptions are visible. As the water rushes down the fore reef, the flow transitions from flux to dispersion-dominated.

These results show that both depth-averaged and fully three-dimensional models can predict these flows. In particular, the agreement between EOLE's, SLOWS' and TUCWave's results for most of the flow is quite surprising. Besides the resolution requirements (definition of the interface), the precise definition of the quantities to be plotted may be in this case quite crucial for this type of flow, and should be related to the experimental uncertainty (unfortunately not available here).

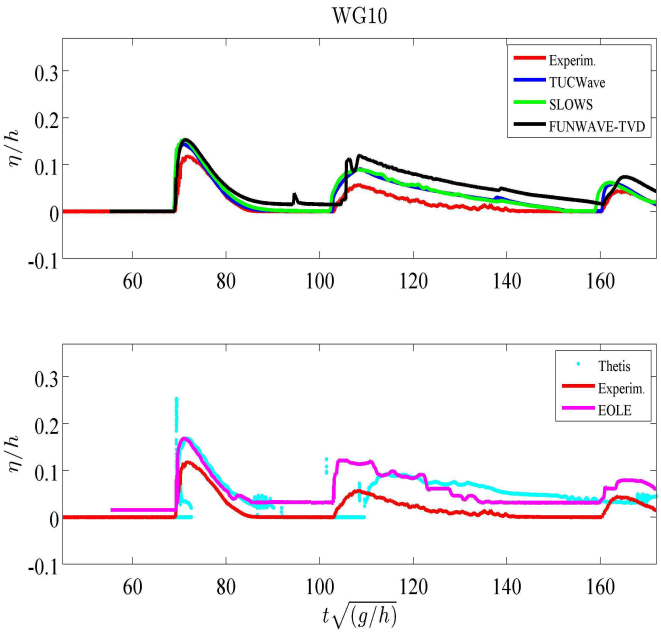

Figure 7c. Continuation of Fig. 7b, WG 10.

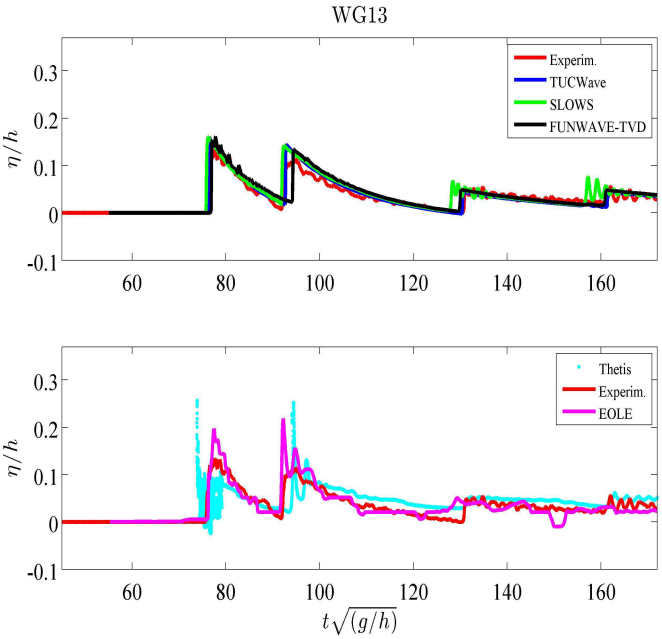

Figure 7d. Continuation of Fig. 7c, WG 13.

Figs. 7a to 7d compare the computed and recorded surface elevation time series at four specific wave gauges. The recorded data from the wave gauges at $x \leq 50.4$m (*i.e.* WGs 2-8) show the effect of the dispersive waves on the free surface. The hydraulic jump developed at the fore reef produces a train of waves

over the increasing water depth and the resulting undulations are intensified as higher harmonics are released. All the Boussinesq-type models provide a quite faithful description of the whole process, including the dispersion dominated process observed before the reef at later times. EOLE provides a good description of the early phase of the process and a somewhat satisfying prediction of the dispersion dominated undular bore, with higher frequency oscillations missing in the results, perhaps due to a lack of resolution. THETIS provides a correct description of the wave propagation, but it gives a late breaking inception with a phase advance of the bore on the reef flat, and a phase lag of the reflected bore. In strongly breaking regions THETIS data is also dominated by very large oscillations which may be related to the post-processing if strong air entrainment is predicted by the VOF code.

4 SEASIDE EXPERIMENT: IMPACT ON A URBAN AREA

4.1 *Case description*

This experimental case has been realized in the Oregon State University basin. A complex topography was built including a seawall and several buildings, inspired of the real city of Seaside (Oregon) at a 1/50 scale. The experiment consisted in generating a solitary wave with a piston-type wavemaker. This wave (height = 0.2m, period = 10s) was designed to correspond to the estimated tsunami wave height for the "500 years" CSZ (Cascadia Subduction Zone) tsunami. The experiment was reproduced 136 times, while displacing the sensors in the urban area (31 locations), and 99 of these trials have been judged as acceptable. As data about flows in an urban area remain very rare, this test-case is particularly interesting to compare the ability of the different models and of the different approaches to simulate the flows in a complex topography.

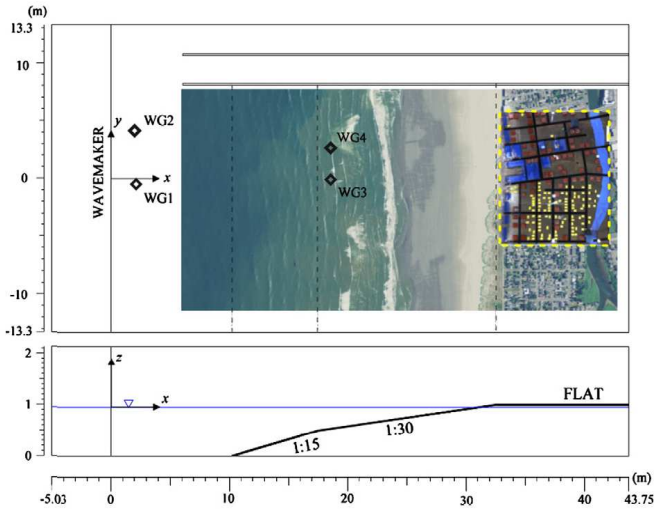

Figure 8. Impact on a urban area: plan view of the experiment in the basin and position of the offshore wave-gauges (up) and cross-section of the theoretical topography (down). Taken from Park *et al.* (2013).

An overview of the experiment is presented in Fig. 8, issued from Park *et al.* (2013). A LiDAR survey has been realized on the main part of the experimental basin (dimensions are 48.8m long, 26.5m wide and 2.1m deep). BRGM has reconstituted an idealized topo-bathymetry based on this LiDAR survey. This idealized topo-bathymetry was used to fill the gaps in the original LiDAR data. Moreover, the topo-bathymetry was vertically moved for an initial water level at the 0-altitude, and horizontally limited to the area of interest. The proposed topo-bathymetry is represented in Fig. 9.

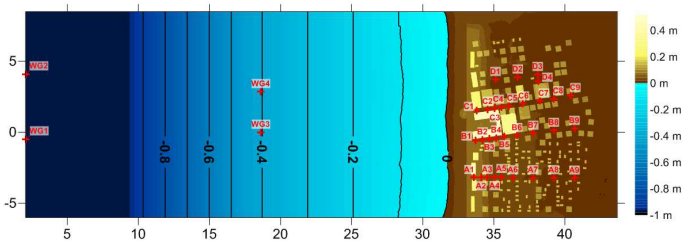

Figure 9. Impact on a urban area: view of the proposed topo-bathymetry and positions of the sensors.

Up, down and right boundaries are supposed to be walls, insofar as this case corresponds to a basin experiment (up- and down-boundaries don't correspond to the basin limits, but available videos show that the urban area was closed by walls). The wave is generated from the left boundary, using the water height measurements on WG1 of Fig. 9 (this implies that the reflected waves are included in the signal). In the experiment, the structure was constructed of smooth concrete with a flat finish, leading to an estimated roughness height of 0.1-0.3 mm. Consequently, a Manning coefficient of 0.010 $m^{-1/3}$.s is suggested.

4.2 *Benchmarking results*

Five codes were tested in this case:
- EOLE (see Section 2.2),
- FUNWAVE-TVD (see Section 3.2),
- Telemac-2D, developed by EDF, solving NLSWE with FE or FV,
- Calypso, developed by CEA, solving NLSWE with Finite Differences,
- SURF-WB, developed by the universities of Bordeaux and Montpellier, solving NLSWE with FV.

Fig. 10 shows time series of the free surface elevation for the five codes and measurements, on four of the gauges shown on Fig. 9. On gauge WG3, located offshore (middle of Fig. 9), all codes are late with respect to the data; this could be explained by a time error on this gauge in the available experimental data (for example, in Rueben *et al.*, 2010, the peak on WG3 appears at about 20s, which is more consistent with the simulations). The delay seems to be larger

with EOLE, the only code solving the Navier-Stokes equations in this case. After the wave reflection on the coast, the experimental data show free-surface oscillations that are only predicted by FUNWAVE-TVD.

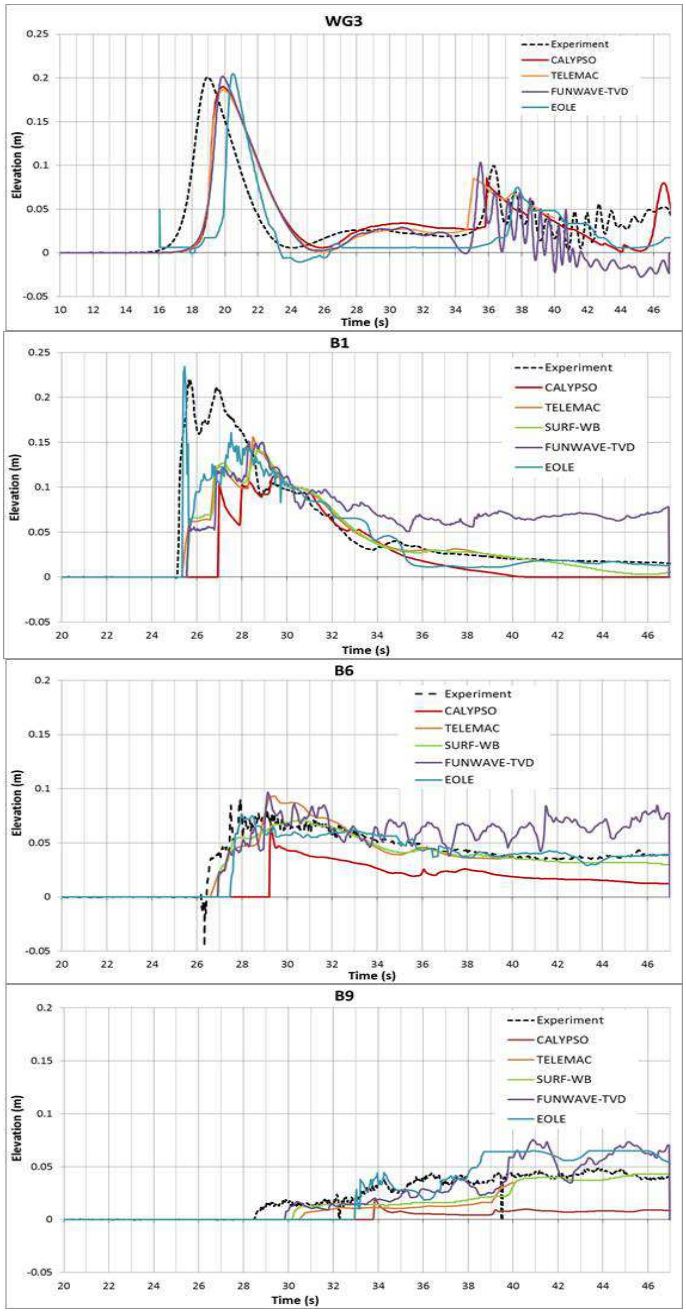

Figure 10. Impact on a urban area: time series of free surface elevation at four gauges. From top to bottom: gauges WG3, B1, B6 and B9 (see Fig. 9). Black dotted lines: experiments by Park *et al.* (2013); light blue lines: EOLE; purple lines: FUNWAVE-TVD; green lines: SURF-WB; orange lines: Telemac-2D; brown lines: Calypso.

For gauges B1, B6 and B9 (located in the city on Fig. 9), all codes perform satisfactorily, reasonably well although differences with experimental data are significant, in particular at gauge B1. On the four gauges, EOLE (Navier-Stokes equations) and Telemac-2D (NLSWE) globally show the lowest differences with data. On B1, the initial free-surface elevation peak is underestimated by all codes, but the subsequent behavior is correctly predicted except by FUNWAVE-TVD (ovestimation) and Calypso (underestimation). Similar conclusions can be drawn for B6. As for B9, the best models are EOLE and FUNWAVE-TVD.

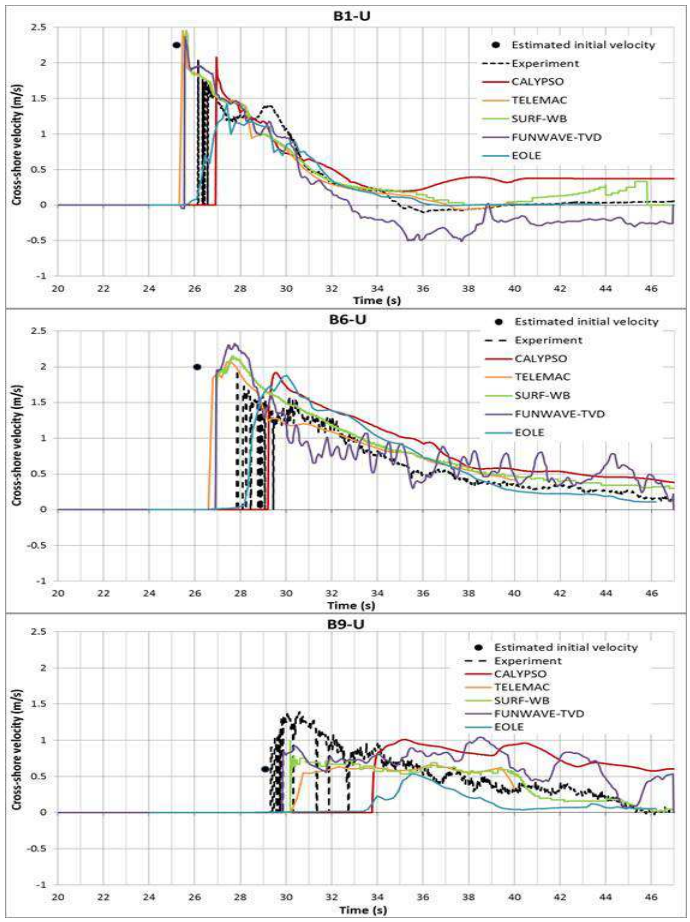

Figure 11. Impact on a urban area: time series of velocity at three gauges. From top to bottom: gauges B1, B6 and B9 (see Fig. 9). Same color code as Fig. 10. The black circle indicates the estimated initial velocity.

In estimating the consequences of tsunami impact, water levels are not sufficient. Fig. 11 shows velocity time series on the same gauges except WG3. The velocities are globally well predicted, even if in long-term Calypso tends to overestimate them and FUNWAVE-TVD simulates a too important reflux near the coastline (in agreement with the abovementioned behavior regarding water elevation). New features under development should improve the Calypso results especially on energy conservation. All codes have difficulties to predict the velocity on gauge B9, the most remote to the initial coastline.

As a conclusion, the use of depth-averaged models (such as NLSWE or Boussinesq-type models) seems to be enough for such cases. Nevertheless, 3D approaches may be interesting in calculating the resulting force on buildings. Fig. 12 shows an example of 3D rendering with EOLE, along with a first simulation obtained with the code Sphynx (see Section 2.2).

5 CONCLUSIONS

We have presented three benchmark cases for testing tsunami simulations on the main three stages: generation, propagation and impact/run-up. Various codes have participated, some using averaging or *a priori* assumptions of the vertical structure of the flow (solving the NLSWE or Boussinesq-type equations), some in 3D (solving the Navier-Stokes equations with free-surface treatment). Most use traditional approaches like FV or FE, one of them is based in SPH. All codes are thus very different, and differences in quality and accuracy of results could be highlighted on most cases of this test bed. Depending on the stage of the tsunami event (generation, propagation, inundation) some of them appear to be most suited, and a complete modelling chain would likely rely on the coupling some of these models (a topic which is also addressed in the Tandem project).

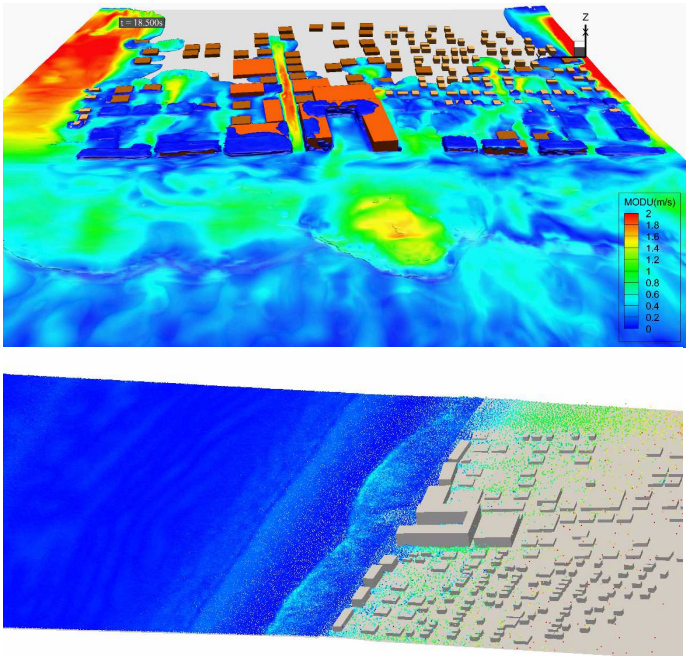

Figure 12. Impact on a urban area: 3D view with EOLE (top) and first simulation with Sphynx (bottom).

In the near future, this case will serve to investigate sensitivity to parameter uncertainty (bed friction, initial conditions, etc.).

6 ACKNOWLEDGMENTS

This work has been done in the framework of the French national research project Tandem, supported by the French government (Projets Investissement d'Avenir, agreement reference number ANR-11-RSNR-0023-01).

7 REFERENCES

Kazolea, M., Delis, A.I., Nikolos, I.K., Synolakis, C.E. 2012. An unstructured finite volume numerical scheme for extended Boussinesq-type equations. *Coast. Engng*. **69**:42–66.

Monaghan, J.J., Kos, A. 2000. Scott Russell's wave generator. *Phys. Fluids* **12**(3):622–630.

Park H., Cox D.T., Lynett P.J., Wiebe D.M., Shin S. 2013. Tsunami inundation modeling in constructed environments: A physical and numerical comparison of free-surface elevation, velocity, and momentum flux. *Coast. Engng*. **79**:9–21.

Ricchiuto, M., Filippini, A.G. 2014. Upwind Residual discretization of enhanced Boussinesq equations for wave propagation over complex bathymetries. *J. Comput. Phys*. **271**:306–341.

Roeber, V. 2010. Boussinesq-type model for nearshore wave processes in fringing reef environment. *PhD Thesis, University of Hawaii*.

Roeber, V., Cheung, K.F. 2012. Boussinesq-type model for energetic breaking waves in fringing reef environments. *Coast. Engng*. **70**:1–20.

Rueben M., Holman R., Cox D., Shin S., Killian J., Stanley J. 2010. Optical measurements of tsunami inundation through an urban waterfront modeled in a large-scale laboratory basin, Coast. Engng. **58**:229–238.

Shi, F., Kirby, J.T., Harris, J.C., Geiman, J.D., Grilli, S.T. 2012. A high-order adaptive time-stepping TVD solver for Boussinesq modeling of breaking waves and coastal inundation. *Ocean Model*. **43-44**:36–51.